A First Order 3-D Finite-Difference Chorin-Temam scheme for Brinkman Equation

A flexible and parallel PETSc Object-Oriented algorithm

Davide Galbiati and Alessandra Gotti

Dipartimento di Matematica (MOX)
Politecnico di Milano

January 25, 2025

Abstract and Introduction

- Development of a parallel multi-physics solver in C++ using PETSc.
- Pre-processing of the carotid artery geometry using VMTK.
- Simulations performed at Reynolds numbers (Re) ranging from 1 to 2000.
- Blood-flow CFDs with a timestep of $1e-3$ and 70 refinements per spatial direction and $Re = [200, 900]$

Advantages and Disadvantages of our Approach

Advantages

- **Finite Differences** for computational efficiency.
- Easy handling of **complex geometries**.
- **Scalability** thanks to pressure-velocity decoupling.
- **Efficiency** thanks to fully explicit non-linear term.

Disadvantages

- Loss of accuracy near boundaries.
- Stability **only** under CFL condition.
- Half-order convergence loss due to **Chorin-Temam**.
- Fully **Dirichlet** boundary conditions not proper for channel flows.

Incompressible Navier-Stokes System

$$\frac{\partial \mathbf{u}}{\partial t} + (\mathbf{u} \cdot \nabla)\mathbf{u} - \nu \Delta \mathbf{u} + \nabla p = \mathbf{f}, \quad \text{in } \Omega \times (0, T) \tag{1}$$

$$\nabla \cdot \mathbf{u} = 0, \quad \text{in } \Omega \times (0, T) \tag{2}$$

$$\mathbf{u} = \mathbf{g}(\mathbf{x}, t), \quad \text{on } \partial\Omega \times [0, T) \tag{3}$$

$$\mathbf{u}(\mathbf{x}, 0) = \mathbf{h}(\mathbf{x}), \quad \text{in } \Omega \tag{4}$$

- $\mathbf{u}$: Velocity field, p: Pressure (divided by density).
- ν: Kinematic viscosity, $\mathbf{f}$: External force ($L^2(\mathbf{R}^+)$).
- $\mathbf{g}(\mathbf{x}, t)$: Prescribed velocity on $\partial\Omega$.
- $\mathbf{h}(\mathbf{x})$: Initial velocity distribution.

Modelling internal blood flow within a carotid artery: the Brinkman Penalization Method

- Domain Ω: A parallelepiped representing the computational region.
- Artery walls embedded defining the "fictitious" sub-domain Ω_ν.
- No-slip boundary condition imposed on $\partial\Omega_\nu$, $\mathbf{u_0} = \mathbf{0}$:

$$\frac{\partial \mathbf{u}}{\partial t} + (\mathbf{u} \cdot \nabla)\mathbf{u} - \nu \Delta \mathbf{u} + \nabla p + \frac{1}{\eta}\chi(\mathbf{x})(\mathbf{u} - \mathbf{u_0}) = \mathbf{f} \quad \text{in } \Omega \times (0, T), \tag{5}$$

$$\nabla \cdot \mathbf{u} = 0 \quad \text{in } \Omega \times (0, T), \tag{6}$$

$$\mathbf{u} = \mathbf{g}(\mathbf{x}, t) \quad \text{on } \partial\Omega_\nu \times [0, T) \quad \mathbf{u} = 0 \quad \text{on } \partial\Omega \setminus \partial\Omega_\nu \times [0, T) \tag{7}$$

$$\mathbf{u} = \mathbf{h}(\mathbf{x}, 0) \quad \text{in } \Omega_\nu \quad \mathbf{u} = 0 \quad \text{in } \Omega \setminus \Omega_\nu \tag{8}$$

Modelling internal blood flow within a carotid artery: the Brinkman Penalization Method

- $\eta > 0 \in \mathbb{R}$ is the penalization coefficient, set at $1e - 6$ for our simulations.
- Characteristic function $\chi(\mathbf{x})$:

$$\chi(\mathbf{x}) = \begin{cases} 0 & \text{if } \mathbf{x} \in \Omega_\nu, \\ 1 & \text{otherwise.} \end{cases}$$

Advantages:

- Simplifies handling complex geometries (e.g., curved walls) using a Cartesian domain.
- Implicitly enforces boundary conditions on the walls of the artery.
- Suitable for Cartesian grids, avoiding mesh triangulation complexities.

Modelling internal blood flow within a carotid artery: the Brinkman Penalization Method

- Conversion of STL file to VTP format.
- Centerlines computation for geometry orientation.
- Flow extensions at inlet and outlet (length = 5*diameter).
- Geometry remeshing (mesh size = 0.5).
- Ray-casting algorithm.

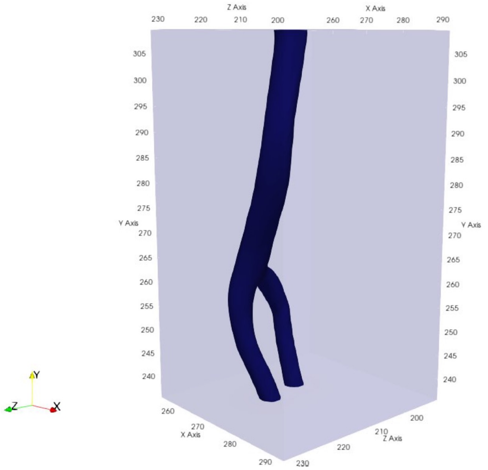

Preprocessing with VMTK Visualization

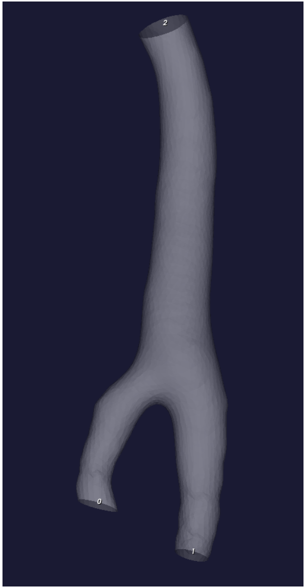

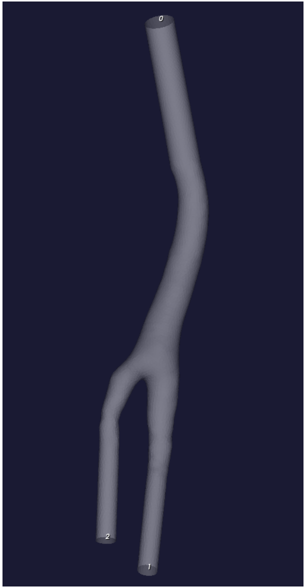

Structured Cartesian Staggered Grid Configuration for Navier-Stokes Equations

Staggered grid for numerical stability thanks to separation of velocity and pressure [Date, 1993].

LEFT and RIGHT faces of the cells for u-velocity.

TOP and BOTTOM faces for v-velocity.

FRONT and BACK faces for w-velocity.

Pressure p defined at cell CENTERS.

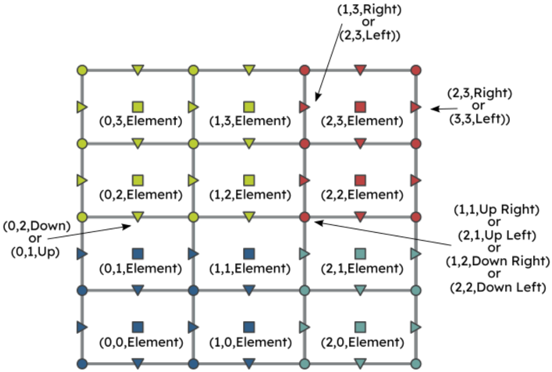

Figure: from petsc.org

Projection Method for the Navier-Stokes Equations: advection-diffusion step

If the advection diffusion operator is split from from the incompressibility constraints, the **projection method** arises. With an appropriate time discretization Δt, the Navier-Stokes system is divided into two steps (here we suppose no source term) [Parolini, 2023]

$$\frac{\mathbf{u}_e^{n+1} - \mathbf{u}^n}{\Delta t} - \nu \Delta \mathbf{u}_e^{n+1} + (\mathbf{u}^n \cdot \nabla)\mathbf{u}^n = 0 \quad \text{in } \Omega \times [t_1 \ldots T], \tag{9}$$

$$\mathbf{u}_e^{n+1} = \mathbf{g}(\mathbf{x}, t_{n+1}) \quad \text{on } \partial\Omega \times [t_1 \ldots T], \quad \mathbf{u}_e^0 = \mathbf{g}(\mathbf{x}, t_0) \quad \text{on } \partial\Omega, \quad n \in [0, T/\Delta t] \tag{10}$$

$$\mathbf{u}_e(\mathbf{x}, 0) = \mathbf{h}(\mathbf{x}) \quad \text{in } \Omega, \tag{11}$$

It inherits the same boundary conditions as the original Navier-Stokes problem, with Dirichlet BCs.

Projection Method for the Navier-Stokes Equations: projection step

$$\frac{\mathbf{u}^{n+1} - \mathbf{u}_e^{n+1}}{\Delta t} + \nabla p^{n+1} = 0, \quad \text{with} \quad \operatorname{div} \mathbf{u}^{n+1} = 0 \quad \text{in } \Omega \times [t_1 \ldots T], \tag{12}$$

$$\mathbf{u}^{n+1} \cdot \mathbf{n} = \mathbf{g}(\mathbf{x}, t_{n+1}) \cdot \mathbf{n} \quad \partial\Omega \times [t_1 \ldots T], \quad \mathbf{u}^0 \cdot \mathbf{n} = \mathbf{g}(\mathbf{x}, t_0) \cdot \mathbf{n} \quad \partial\Omega, \quad n \in [0, T/\Delta t] \tag{13}$$

$$\mathbf{u}(\mathbf{x}, 0) = \mathbf{h}(\mathbf{x}) \quad \text{in } \Omega, \tag{14}$$

$$\mathbf{u}^{n+1} = \mathbf{u}_e^{n+1} - \Delta t \nabla p^{n+1}. \tag{15}$$

The second step involves the pressure projection in the H_{div} space, where only the normal component of the velocity can be defined on the boundary. Hence a splitting error arises due to the projection method, as the velocity trace on the boundary is not fully defined [Ferrero et al., 2013], [Parolini, 2023]

Poisson Problem for the Pressure Field

In the second step of the projection method, the pressure field p^{n+1} can be efficiently solved as an elliptic problem. By applying the divergence operator to the first equation, we get:

$$\operatorname{div}\left(\frac{\mathbf{u}^{n+1}-\mathbf{u}_e^{n+1}}{\Delta t}+\nabla p^{n+1}\right)=\operatorname{div}(\mathbf{u}^{n+1})-\operatorname{div}(\mathbf{u}_e^{n+1})+\operatorname{div}(\nabla p^{n+1})=0. \tag{16}$$

This leads to the following Poisson equation for the pressure p^{n+1}:

$$\Delta p^{n+1}=\frac{1}{\Delta t}\operatorname{div}(\mathbf{u}_e^{n+1}). \tag{17}$$

Elliptic Problem for the Pressure Field

To derive the boundary condition for this equation, we consider the normal component of the first equation evaluated on the boundary:

$$\frac{1}{\Delta t}\left(\mathbf{u}^{n+1}\cdot\mathbf{n}-\mathbf{u}_e^{n+1}\cdot\mathbf{n}\right)+\nabla p^{n+1}\cdot\mathbf{n}=0 \quad \text{on } \partial\Omega. \tag{18}$$

Since both velocities are equal to $\mathbf{g}\cdot\mathbf{n}|_{\partial\Omega}$, we obtain a homogeneous Neumann boundary condition for the pressure:

$$\frac{\partial p^{n+1}}{\partial \mathbf{n}}=0. \tag{19}$$

Remark: compatibility condition will be enforced, through conservative bc's.

We assume appropriate boundary and initial conditions, considering the domain subdivision into Ω_ν and $\Omega \setminus \Omega_\nu$.

$$\frac{\mathbf{u}_{e_1} - \mathbf{u}^n}{\Delta t} + (\mathbf{u}^n \cdot \nabla)\mathbf{u}^n = 0, \quad \text{in } \Omega \times [t_1 \ldots T] \tag{20}$$

$$\mathbf{u}_{e_1} = \mathbf{g}(\mathbf{x}, t_{n+1}) \quad \text{on } \partial\Omega \times [t_0 \ldots T] \tag{21}$$

$$\mathbf{u}_{e_1}(\mathbf{x}, 0) = \mathbf{h}(\mathbf{x}) \quad \text{in } \Omega \tag{22}$$

Brinkman Model in the Projection Method Framework

$$\frac{\mathbf{u}_{e_2} - \mathbf{u}_{e_1}}{\Delta t} - \nu \Delta \mathbf{u}_{e_2} + \frac{1}{\eta}\chi(\mathbf{x})(\mathbf{u}_{e_2}) = 0, \quad \text{in } \Omega \times [t_1 \ldots T], \tag{23}$$

$$\mathbf{u}_{e_2} = \mathbf{g}(\mathbf{x}, t_{n+1}) \quad \text{on } \partial\Omega \times [t_0 \ldots T] \tag{24}$$

$$\mathbf{u}_{e_2}(\mathbf{x}, 0) = \mathbf{h}(x) \quad \text{in } \Omega \tag{25}$$

$$\Delta p^{n+1} = \frac{1}{\Delta t} \operatorname{div} \mathbf{u}_{e_2}, \quad \text{in } \Omega \tag{26}$$

$$\frac{\partial p^{n+1}}{\partial \mathbf{n}} = 0, \quad \text{on } \partial\Omega \tag{27}$$

$$\mathbf{u}^{n+1} = \mathbf{u}_{e_2} - \Delta t \nabla p^{n+1} \tag{28}$$

Spatial Discretization: Convective Term

Discretization on k-th Cell as in [Seibold, 2008]:

$$\mathbf{u}_k^n \cdot \nabla u_k^n = \frac{(u^n)_{k+1}^2 - (u^n)_{k-1}^2}{h_x} + \frac{(u^n v^n)_{k+1} - (u^n v^n)_{k-1}}{h_y} + \frac{(u^n w^n)_{k+1} - (u^n w^n)_{k-1}}{h_z},$$

$$\mathbf{u}_k^n \cdot \nabla v_k^n = \frac{(v^n)_{k+1}^2 - (v^n)_{k-1}^2}{h_y} + \frac{(v^n u^n)_{k+1} - (v^n u^n)_{k-1}}{h_x} + \frac{(v^n w^n)_{k+1} - (v^n w^n)_{k-1}}{h_z},$$

$$\mathbf{u}_k^n \cdot \nabla w_k^n = \frac{(w^n)_{k+1}^2 - (w^n)_{k-1}^2}{h_z} + \frac{(w^n u^n)_{k+1} - (w^n u^n)_{k-1}}{h_x} + \frac{(w^n v^n)_{k+1} - (w^n v^n)_{k-1}}{h_y}.$$

Spatial Discretization: Interpolation for Non-linear (Linearized) Terms

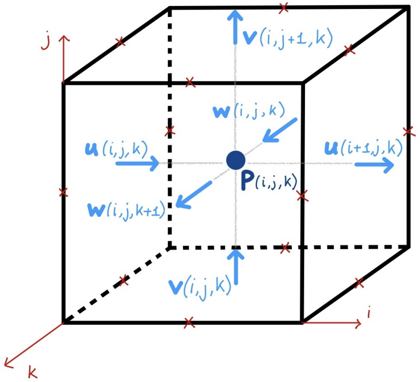

- For mixed components, interpolation happens on edges and the central scheme re-places the field on the correct DoF.
- For homogeneous components, interpolation happens in the cell centres and the central scheme re-places the field on the correct DoF, ($\xi = \eta$).

Spatial Discretization: Laplacian Approximation

$$\Delta u(x,y,z) \approx \frac{u(x-h,y,z) - 2u(x,y,z) + u(x+h,y,z)}{h^2} + \frac{u(x,y-h,z) - 2u(x,y,z) + u(x,y+h,z)}{h^2} + \frac{u(x,y,z-h) - 2u(x,y,z) + u(x,y,z+h)}{h^2}.$$

Dirichlet conditions imposed at $h/2$ distance from the domain faces applied on faces alligned with the components.

For Neumman homogeneous problem corrections applied for pressure near boundaries.

$$p''(x,y,z) \approx \frac{-p(x,y,z) + p(x+h,y,z)}{h^2}.$$

Stability Analysis: The Convective Problem Constraint

Explicit Convective problem (CT 1st-step) is stable under CFL condition [Parolini, 2023]

$$\Delta t \leq C \frac{h}{\|\mathbf{u}\|_\infty},$$

where:

- h: Spatial grid size.
- $\|\mathbf{u}\|_\infty$: Maximum velocity.
- C: Positive constant.

This ensures numerical solution remains stable, i.e. oscillatory instability or uncontrolled error growth. As CFL dictates, explicit step requires careful handling for high-velocity flows or fine grids.

Stability Analysis: The Implicit Parabolic Problem

Implicit problem is expected to be stable. The proof is carries out by Von Neumann Analysis that is particularly suited for Finite-Differences approach.

$$\frac{\hat{e}_k}{\tilde{e}_k} = \frac{1}{1 + 4\frac{h^2}{\nu}\sin^2\left(\frac{kh}{2}\right) + \frac{\chi}{\eta}}.$$

Defined the amplification factor:

$$G \equiv \frac{\hat{e}_k}{\tilde{e}_k},$$

the stability criterion is fulfilled:

$$|G| \leq 1.$$

Convergence Estimates in Time

The time convergence of the present scheme is stated in [Guermond et al., 2006]

$$\|u^n - u_{\mathrm{ex}}\|_{L^2(\Omega)^d} \leq C(u, p, T)\Delta t,$$

$$\|p^n - p_{\mathrm{ex}}\|_{L^2(\Omega)^d} \leq C(u, p, T)\Delta t^{1/2}.$$

Convergence Estimate in Space

Here the objective is to prove second-order spatial convergence for 3D-staggered grids. For the non-linear term, leveraging 2nd-order Taylor expansions it can be shown that:

$$|e(\chi)| \leq \frac{1}{4} \cdot h^2 \left(|\eta' \xi'' + \eta'' \xi'| \right),$$

proving second-order convergence for staggered stencils. Homogeneous terms ($\eta = \xi$) follow the same proof structure.

For the three point stencil both in Dirichlet and fully-Neumann problem we gain an estimate like:

$$|e(\chi)| \leq \frac{h^2}{6} |\xi^{(4)}(\chi)|.$$

The conclusion is that the overall method maintains second-order spatial convergence.

Matrix Structure in PETSc Implementation

Matrix entries are set using a grid-aware structure, simplifying the implementation of complex operations.

For the parabolic problem, imagined in a 1D scheme the matrix would be:

$$L = \frac{1}{h^2}\begin{bmatrix} val & 1 & 0 & \cdots & 0 \\ 1 & val & 1 & \cdots & 0 \\ 0 & 0 & 1 & \cdots & 0 \\ \vdots & \vdots & \vdots & \ddots & \vdots \\ 0 & 0 & 0 & \cdots & 1 \\ 0 & 0 & 0 & \cdots & val \end{bmatrix}$$

Main diagonal: $val = -2 - \frac{h^2}{dt\nu} - \frac{h^2\chi}{\eta\nu}$.

Boundary conditions are directly applied, modifying the first and last rows, while bc's values got to rhs.

This ensures boundary conditions are integrated into the solution, but breaks symmetry.

Matrix Structure in PETSc Implementation

For a 1D Laplacian with Neumann boundary conditions:

$$L = \frac{1}{h^2} \begin{bmatrix} -1 & 1 & 0 & \cdots & 0 & \\ 0 & 1 & 0 & \cdots & 0 & \\ 0 & 1 & -2 & 1 & \cdots & 0 \\ \vdots & \vdots & \vdots & \ddots & \vdots & \\ 0 & 0 & 0 & \cdots & -1 & 1 \end{bmatrix}$$

The first and last rows enforce zero-flux boundary conditions.

No change of rhs is required. Instead a node is fixed to 1. This fixes the problem to a constant but breaks the symmetry.

Solver choice and Preconditioning

- Non-symmetric large problems solved using GMRES (Generalized Minimal Residual).
- Exact solution is guaranteed in at most N steps (Cayley-Hamilton theorem) [Parolini, 2023]
- Preconditioning improves convergence by transforming the system.
- Diagonal preconditioner performs best for the parabolic problem.
- Block-diagonal preconditioner for pressure matrix:

$$M = \mathrm{diag}(A_{11}, A_{22}, \ldots, A_{kk}),$$

  where A_{ij} are blocks of A.
- Preconditioned systems read:

$$M^{-1}AU = M^{-1}F.$$

Analytical Solution for Validation

$$
\begin{aligned}
u &= -a\left[e^{ax}\sin(ay+dz) + e^{az}\cos(ax+dy)\right]e^{-d^2 t},\\
v &= -a\left[e^{ay}\sin(az+dx) + e^{ax}\cos(ay+dz)\right]e^{-d^2 t},\\
w &= -a\left[e^{az}\sin(ax+dy) + e^{ay}\cos(az+dx)\right]e^{-d^2 t},\\
p &= -\frac{a^2}{2}\Bigg[e^{2ax} + e^{2ay} + e^{2az} + 2\sin(ax+dy)\cos(az+dx)e^{a(y+z)}\\
&\qquad + 2\sin(ay+dz)\cos(ax+dy)e^{a(z+x)} + 2\sin(az+dx)\cos(ay+dz)e^{a(x+y)}\Bigg]e^{-2d^2 t}.
\end{aligned}
$$

Fully 3D analytical solution to the Navier-Stokes equations ([Ethier and Steinman, 1994]), depends on all three Cartesian coordinates.

Cube domain: $[-0.5, 0.5]^3$, parameters: $a = \frac{\pi}{4}$, $d = \frac{3\pi}{2}$.

Convergence Analysis: Time (Velocity), Re $= 1$

- First-order time convergence observed as expected.
- Initial $dt = 0.00625$, halved iteratively.
- High spatial refinement ensures time convergence trend is not masked.
- Same results for v, w

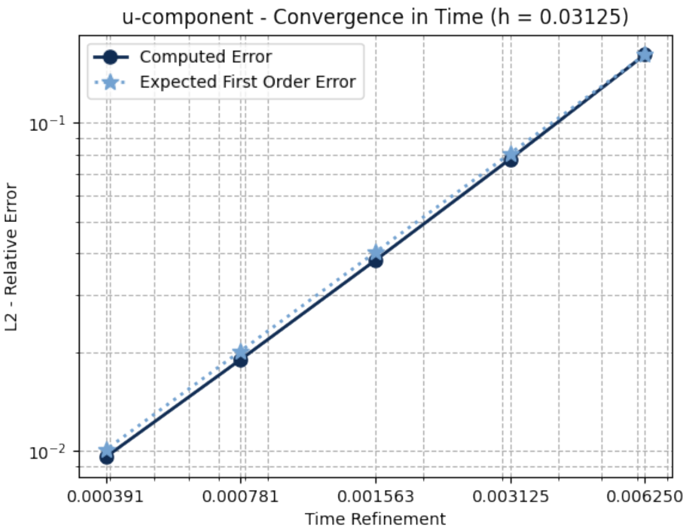

Convergence Analysis: Time (Pressure), Re $= 1$

- Time convergence for pressure confirmed at 0.5 rate.
- Higher error compared to velocity due to pressure constant differences.

  Analytical pressure fixed to 0; numerical uses a shifted constant (hence stagnation)

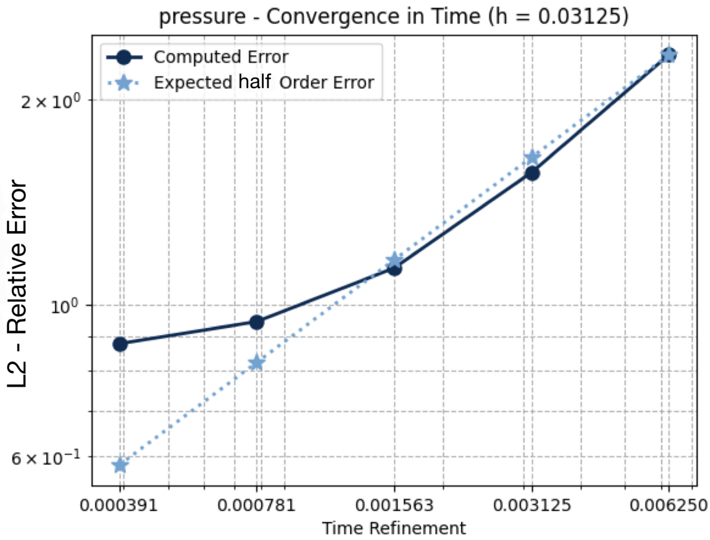

Convergence Analysis: Space (First Attempt), Re $= 1$

- Small time step ($dt = 1.95313 \times 10^{-4}$) to respect CFL condition.
- Spatial convergence observed initially (second order).
- Stagnation due to time discretization error masking true trend.

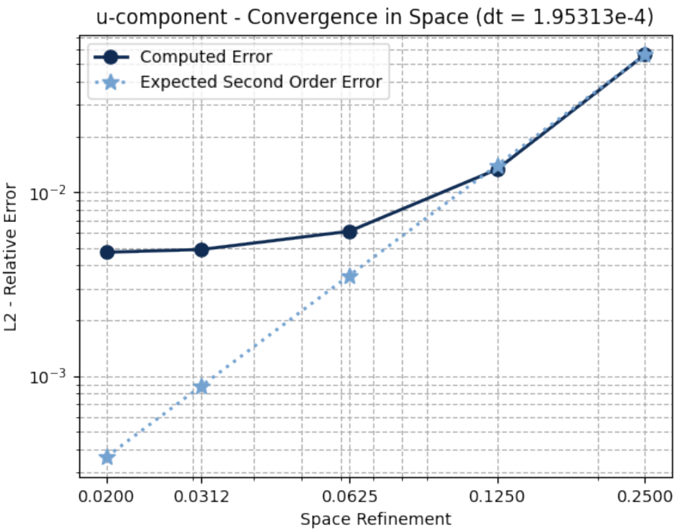

Convergence Analysis: Space (Refined Attempt), Re $= 1$

- Time step further reduced to refine results and make space trend emerge.
- Errors decrease, aligning closer to expected convergence trend.
- Stagnation still present but results indicate reliability.

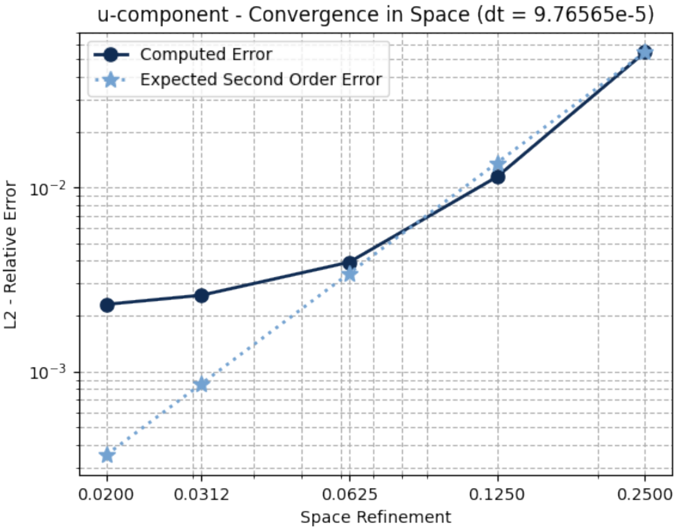

Final NS Simulation: Re = 1, 2000 h = 1/32, dt = 5e-4

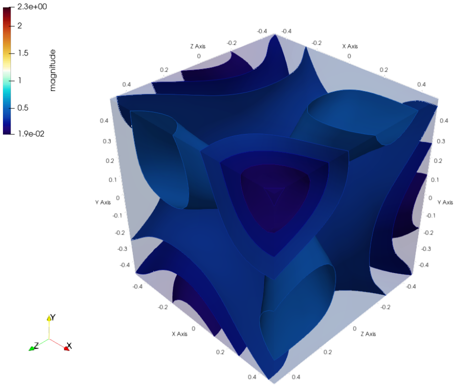

Magnitude at Re = 1, T = 0.015, h = 1/32

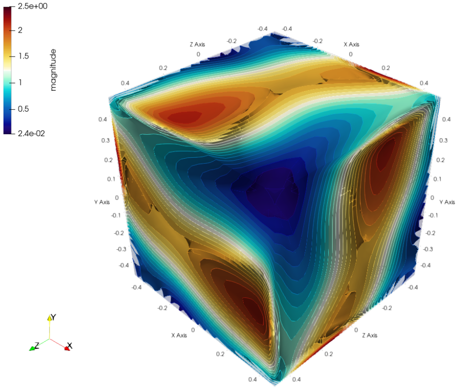

Magnitude at Re = 2000, T = 0.015, h = 1/32

Final Brinkman Simulation: Re = 200, dt = 1e-3, on a grid 70x70x70

$$\int_{S_{\text{in}}} \mathbf{v} \cdot \mathbf{n} \, dA + \int_{S_{\text{out1}}} \mathbf{v} \cdot \mathbf{n} \, dA + \int_{S_{\text{out2}}} \mathbf{v} \cdot \mathbf{n} \, dA = 0 \tag{29}$$

- S_{in}: Area $= 25.6$ ($2.56e1\,\mathrm{mm}^2$), velocity $= (0, -1, 0)$
- S_{out1}: Area $= 10.7$ ($1.07e1\,\mathrm{mm}^2$), velocity $= (0, -1.20, 0)$
- S_{out2}: Area $= 10.8$ ($1.08e1\,\mathrm{mm}^2$), velocity $= (0, -1.18, 0)$

- Characteristic velocity: $1.33e-1\,\mathrm{m/s}$.
- Blood kinematic viscosity: $\nu = 3.8e-6\,\mathrm{m}^2/\mathrm{s}$.
- Dimensional time: $4.39e-2\,\mathrm{s}$.

Final Brinkman Simulation: Re = 200, dt = 1e-3, on a grid 70x70x70

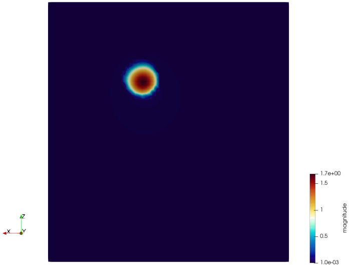

Magnitude at Re = 1, T = 0.015, h = 1/32

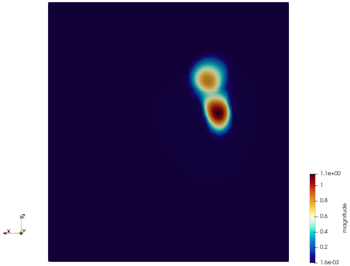

Magnitude at Re = 200, T = 0.015, h = 1/32

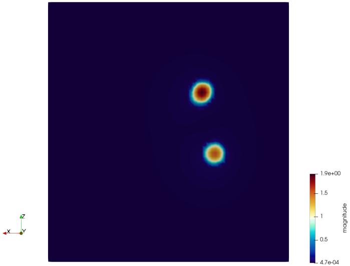

Magnitude at Re = 2000, T = 0.015, h = 1/32

References

Date, A. W. (1993).
Solution of navier-stokes equations on non-staggered grid.
International Journal of Heat and Mass Transfer, 36(7):1913–1922.

Ethier, C. R. and Steinman, D. A. (1994).
Exact fully 3d navier-stokes solutions for benchmarking.
International Journal for Numerical Methods in Fluids, 19:369–375.

Ferrero, A., Gazzola, F., and Zanotti, M. (2013).
Elements of Advanced Mathematical Analysis for Physics and Engineering.
Ed. Esculapio.

Guermond, J. L., Minev, P., and Shen, J. (2006).
An overview of projection methods for incompressible flows.
Computer Methods in Applied Mechanics and Engineering, 195:6011–6045.
Received 10 June 2004; revised 22 August 2005; accepted 21 October 2005.

Parolini, N. (2023).
Computational fluid dynamics course notes.
Politecnico di Milano, September 2023.

Seibold, B. (2008).
A compact and fast matlab code solving the incompressible navier-stokes equations on rectangular domains.

Thank you for your attention!

Compatibility Condition for the Pressure Field

To guarantee well-posedness of homogeneous Neumann Poisson problem compatibility condition must be enforced [Ferrero et al., 2013]:

$$\int_{\Omega} \Delta p^{n+1} \, d\Omega = \int_{\Omega} \frac{1}{\Delta t} \operatorname{div} \mathbf{u}_e \, d\Omega. \tag{30}$$

Hence

$$0 = \int_{\partial\Omega} \frac{\partial p^{n+1}}{\partial \mathbf{n}} \, dS = \int_{\Omega} \frac{1}{\Delta t} \operatorname{div} \mathbf{u}_e \, d\Omega = \int_{\partial\Omega} g \cdot \mathbf{n} \, d\Omega \tag{31}$$

Incompressibility of intermediate field is NOT necessary for well-posedness.

This condition ensures mass (0-flux condition).

The pressure field solution is determined up to a constant, fixing a grid-node is necessary. This implies loss of a target pressure field.

Iterative Solvers: GMRES

- Non-symmetric problems solved using GMRES (Generalized Minimal Residual).
- **Key principles:**
  - Krylov space $K_k(A, R_0) = \text{span}\{R_0, AR_0, \ldots, A^{k-1}R_0\}$.
  - Residual minimized at each iteration:

$$\|R_k\| = \min_{p_k \in P_k} \|p_k(A)R_0\|,$$

  where p_k is a polynomial of degree k and

$$\|R_k\| \leq K(A) \min_{p_k \in P_k} \max_i |p_k(\lambda_i)| \, \|R_0\|,$$

- Exact solution is guaranteed in at most N steps (Cayley-Hamilton theorem) [Parolini, 2023]

Stability Analysis: The Implicit Parabolic Problem

Implicit problem is expected to be stable. The proof is carries out by Von Neumann Analysis that is particularly suited for Finite-Differences approach.

Key-idea: evaluates amplification of Fourier modes in the error.

Leveraging the linearity of the problem and defining the error:

$$e_k = u_k - u_{ex,k}.$$

Substituting into the governing equation:

$$\hat{e_k} - \tilde{e_k} = \frac{1}{\nu} \frac{\widehat{e_{k+1}} - 2\hat{e_k} + \widehat{e_{k-1}}}{h^2} - \frac{\chi}{\eta} \hat{e}.$$

Error Evolution and Stability Criterion

From Inverse-Transform definition which is

$$e(x,t) = \int_{-\infty}^{\infty} E_k(t) e^{ikx} \, dk,$$

where $E_k(t)$ governs error evolution one obtains for the integrands:

$$\frac{\hat{e}_k}{\tilde{e}_k} = \frac{1}{1 + 4\frac{h^2}{\nu}\sin^2\left(\frac{kh}{2}\right) + \frac{\chi}{\eta}}.$$

Defined the amplification factor:

$$G \equiv \frac{\hat{e}_k}{\tilde{e}_k},$$

the stability criterion is fulfilled:

$$|G| \leq 1.$$